

# Accretion Discs in Blazars

E.J.D. Jolley<sup>1\*</sup>, Z. Kuncic<sup>1</sup>, G.V. Bicknell<sup>2</sup> and S. Wagner<sup>3</sup>

<sup>1</sup>*School of Physics, University of Sydney, Sydney NSW 2006, Australia*

<sup>2</sup>*Research School of Astronomy and Astrophysics, Australian National University, Canberra, Australia*

<sup>3</sup>*Landessternwarte Heidelberg, Konigstuhl, Heidelberg, Germany*

## ABSTRACT

The characteristic properties of blazars (rapid variability, strong polarization, high brightness) are widely attributed to a powerful relativistic jet oriented close to our line of sight. Despite the spectral energy distributions (SEDs) being strongly jet-dominated, a "big blue bump" has been recently detected in sources known as flat spectrum radio quasars (FSRQs). These new data provide a unique opportunity to observationally test coupled jet-disc accretion models in these extreme sources. In particular, as energy and angular momentum can be extracted by a jet magnetically coupled to the accretion disc, the thermal disc emission spectrum may be modified from that predicted by the standard model for disc accretion. We compare the theoretically predicted jet-modified accretion disc spectra against the new observations of the "big blue bump" in FSRQs. We find mass accretion rates that are higher, typically by a factor of two, than predicted by standard accretion disc theory. Furthermore, our results predict that the high redshift blazars PKS 0836+710, PKS 2149-307, B2 0743+25 and PKS 0537-286 may be predominantly powered by a low or moderate spin ( $a \leq 0.6$ ) black hole with high mass accretion rates  $\dot{M}_a \approx 50 - 200 M_\odot \text{ yr}^{-1}$ , while 3C 273 harbours a rapidly spinning black hole ( $a = 0.97$ ) with  $\dot{M}_a \approx 20 M_\odot \text{ yr}^{-1}$ . We also find that the black hole masses in these high redshift sources must be  $\geq 5 \times 10^9 M_\odot$ .

**Key words:** accretion discs — black hole physics — (galaxies:) BL Lacertae objects: individual (3C 273, B2 0743+25, PKS 0537-286, PKS 0836+710, PKS 2149-307) — galaxies: jets.

## 1 INTRODUCTION

Blazars are radio-loud active galactic nuclei (AGN), believed to consist of an accretion disc surrounding a super-massive black hole with a relativistic jet aligned closely with our line of sight (e.g. Urry & Padovani 1995). They are highly luminous at all wavelengths, with rapid variability timescales and relativistic jets. The Spectral Energy Distribution (SED) of a typical blazar consists of a broadband component attributed to synchrotron and inverse Compton emission from relativistic electrons in a jet. The "blazar luminosity sequence" indicates that the high energy peak moves to higher energies for blazars with lower bolometric luminosities (Fossati et al. 1998; Ghisellini et al. 1998).

A new optical-UV component has recently been identified in a growing number of blazars (see Perlman et al. 2008 for a review), particularly flat spectrum radio quasars (FSRQs) and optically violent variables (OVVs). This component has been interpreted as thermal in origin because it exhibits different spectral characteristics from the rest of the SED. This is consistent with the big blue bump (BBB) feature that is seen in quasars and other AGN and commonly attributed to an accretion disc (see e.g. Shang et al.

2005). The thermal disc emission has been difficult to detect in blazars, presumably due to obscuration by the strongly beamed non-thermal emission from the relativistic jet aligned closely with our line of sight. However, if the source is in a faint state, it may be possible to detect the big blue bump, as in the case of 3C 454.3 (e.g. Raiteri et al. 2007) and 3C 273.

Standard accretion disc theory (Pringle & Rees 1972; Novikov & Thorne 1973; Shakura & Sunyaev 1973) assumes that all of the accretion power  $P_a$  is locally radiated in the accretion disc, so that the disc luminosity is  $L_d = P_a$ . The universality of jets, observed across an extraordinary range of accreting sources, including non-relativistic sources (e.g. young stellar objects) and non-spinning sources (e.g. neutron stars), suggests that jets may be efficiently powered by accretion, without the need to invoke black hole spin. Magnetic surface torques can extract energy and angular momentum vertically from an accretion disc to form jets (Blandford & Payne 1982). This results in a dimmer and redder disc spectrum, and a higher mass accretion rate compared to that predicted by standard accretion disc theory (Kuncic & Bicknell 2004, 2007a,b; Jolley & Kuncic 2008a,b). In blazars, the ratio of the disc luminosity  $L_d$  to the jet power  $P_j$  is typically 1 – 10% for cases where both values can be estimated reasonably accurately (Tavecchio et al. 2000; Maraschi & Tavecchio 2003). This implies that more than 90% of the total accretion power can be extracted

\* E-mail: erin@physics.usyd.edu.au

by the jet, leaving less than 10% of the accretion power to be radiated by the disc ( $L_d \approx 0.1P_a$ ). Because blazars exhibit such powerful relativistic jets, the accretion disc emission should be strongly modified, making these sources ideal candidates for detecting jet-modified disc accretion. The black hole mass  $M$  and mass accretion rates  $\dot{M}_a$  of these sources could be substantially higher than that inferred from standard accretion disc theory if the jets are accretion-powered (Jolley & Kuncic 2008a).

In this paper, we model the jet-modified thermal disc emission and synchrotron jet emission in a sample of FSRQs which exhibit a big blue bump (BBB). The high energy emission due to Compton processes is not modelled here; we defer this to future work. We derive key physical accretion parameters such as dimensionless black hole spin  $a$ , black hole mass  $M$  and mass accretion rate  $\dot{M}_a$ . In Section 2, we present our jet-modified accretion disc and synchrotron jet model. This model is applied to 3C 273 in Section 3, and, in Section 4, to four high redshift FSRQs, PKS 0836+710, PKS 2149-307, B2 0743+25 and PKS 0537-286, which were recently detected with SWIFT. Our conclusions are presented in Section 5.

## 2 JET-MODIFIED ACCRETION THEORY

In this section, we present an explicit model for the magnetic coupling between an accretion disc and jet, resulting in a modified disc spectrum (Jolley & Kuncic 2008a). Standard accretion disc theory (Shakura & Sunyaev 1973) predicts the following radiative flux from an accretion disc

$$F(x) = \frac{3GM\dot{M}_a}{8\pi x^3 r_g^3} \left[ 1 - \left( \frac{x_i}{x} \right)^{1/2} \right] \quad (1)$$

where  $G$  is the gravitational constant,  $r_g = GM/c^2$  is the gravitational radius,  $x = r/r_g$  is the dimensionless radius and  $x_i$  is the dimensionless last marginally stable orbit. The disc flux can be generalized by including a relativistic correction term  $f^{\text{NT}}$  (Novikov & Thorne 1973; Page & Thorne 1974) and by including a torque at the inner-most radial boundary  $f^r$  (Agol & Krolik 2000), as well as a torque across the disc surface  $f^z$  (Kuncic & Bicknell 2004; see Jolley & Kuncic 2008a for further details). Thus, the generalized radiative disc flux for a black hole with mass  $M$  and accretion rate  $\dot{M}_a$  can be expressed as:

$$F(x) = \frac{3GM\dot{M}_a}{8\pi x^3 r_g^3} \left[ f^{\text{NT}} + f^r(x) - f^z(x) \right] \quad (2)$$

The torque acting at  $x_i$  does work on the inner-most boundary of the accretion disc and acts to enhance the disc flux at small radii. Conversely, the surface torque does work against the disc, hence reducing the disc flux. It can remove energy from the disc and direct it vertically to form a magnetized jet (Kuncic & Bicknell 2004). A magnetic surface torque can also drive a mass-loaded disc wind at larger radii (see Kuncic 1999), but for simplicity we assume negligible mass loss and hence  $\dot{M}_a$  remains constant at all radii.

Global energy conservation requires the total accretion power  $P_a$  to equal the sum of the total disc radiative power  $L_d$  and the Poynting power removed from the disc to form the jet  $P_j$ :

$$P_a = L_d + P_j \quad (3)$$

Thus the disc radiative efficiency is

$$\epsilon_d = \epsilon_a - \epsilon_j = \epsilon_{\text{NT}} + \epsilon_r - \epsilon_j \quad (4)$$

where  $\epsilon_a$  is the total accretion efficiency,  $\epsilon_{\text{NT}}$  and  $\epsilon_r$  are the efficiencies due to relativistic accretion and the inner boundary torque,

respectively, and  $\epsilon_j$  is the jet efficiency. The efficiencies are defined as

$$\epsilon = \frac{3}{2} \int_{x_i}^{\infty} x^{-2} f(x) dx \quad (5)$$

enabling us to normalise the local torques in terms of their corresponding global efficiencies.

The mass accretion rate can be written as

$$\dot{M}_a = \frac{L_d}{\epsilon_d c^2} \quad (6)$$

and we define the dimensionless mass accretion rate as

$$\dot{m} = \frac{\dot{M}_a c^2}{L_{\text{Edd}}} = \left( \frac{L_d}{L_{\text{Edd}}} \right) \frac{1}{\epsilon_d} \quad (7)$$

where  $L_{\text{Edd}} = 4\pi GMm_p c / \sigma_T$  is the Eddington luminosity. Note that our definition of  $\dot{m}$  does not assume  $\epsilon_d = 0.1$ .

The input parameters for our modified accretion disc model are the fractional efficiency of the torque at the inner boundary  $\epsilon_r/\epsilon_{\text{NT}}$ , the dimensionless black hole spin parameter  $a$  and the fraction of accretion power injected into the jet,  $\epsilon_j/\epsilon_a$ . This last parameter has an upper limit in order that the disc flux remains positive at all radii. The higher the black hole spin, the greater  $\epsilon_j/\epsilon_a$  can be as there is more accretion power available to extract to the jet. The value of  $\epsilon_r/\epsilon_{\text{NT}}$  also determines how large  $\epsilon_j/\epsilon_a$  can be. For  $a = 0$ , we set  $\epsilon_r/\epsilon_{\text{NT}} = 0.05$  (see e.g. Agol & Krolik 2000), allowing  $\epsilon_j/\epsilon_a = 0.50$ . For  $a = 0.97$ ,  $\epsilon_r/\epsilon_{\text{NT}} = 0.10$  so that  $\epsilon_j/\epsilon_a = 0.90$ .

The magnetic torque acting across the disc surface can extract power from the disc and inject it into the jet. Some of the particles are then accelerated to nonthermal, relativistic energies. Consequently, synchrotron radiation by relativistic electrons can contribute significantly to the broadband emission.

The relativistic jet is modelled with a bulk Lorentz factor  $\Gamma_j$  and Doppler factor  $\delta = \left\{ \Gamma_j \left[ 1 - (1 - \Gamma_j^{-2})^{1/2} \cos \theta_j \right] \right\}^{-1}$ , where  $\theta_j$  is the angle between our line of sight and the jet axis. The jet geometry is shown in Figure 1. The initial jet radius is  $r_{j,0} = z_0 \tan(\Gamma_j^{-1})$ , where  $z_0$  is the starting height of the radio-synchrotron jet, and  $\Gamma_j^{-1}$  is the jet half-opening angle (see Blandford & Königl 1979). The jet is divided into cylindrical sections, and the contribution from each component is integrated to give the total emission spectrum. The observed specific luminosity due to the net contribution from each jet component is (see also Jolley & Kuncic 2008a; Freeland et al. 2006):

$$L_\nu^{\text{obs}} \approx 2 \int_{z_0}^{z_j} 4\pi \delta^3 S_\nu^{\text{syn}} (1 - e^{-\tau_\nu^{\text{syn}}}) \pi r \sin \theta_j dz \quad (8)$$

where  $S_\nu^{\text{syn}}$  is the synchrotron source function and

$$\tau_\nu^{\text{syn}} = \delta^{-1} \kappa_\nu^{\text{syn}} \Delta s$$

is the synchrotron optical depth along a path length  $\Delta s \approx 2r / \cos \theta_j$ , where  $r \approx z\phi$ , through each cylindrical section.

The equipartition factor  $f_{\text{eq}} = U_B / U_e$  relates the magnetic field energy density  $U_B = B^2 / 8\pi$  to the relativistic electron energy density  $U_e = \frac{4}{3} \langle \gamma \rangle N_e m_e c^2$ , where  $\langle \gamma \rangle$  is the average Lorentz factor. The proper electron number density  $N_e$  and magnetic field strength  $B$  decline with jet height  $z$  according to  $N_e(z) \propto z^{-2}$  and  $B(z) \propto z^{-1}$ . The total jet power in the observer frame is

$$P_j^{\text{obs}} \approx \pi r_j^2 \Gamma_j (1 - \Gamma_j^{-2})^{1/2} c \times \left[ (\Gamma_j - 1) N_e m_p c^2 + \frac{4}{3} \Gamma_j N_e \langle \gamma \rangle m_e c^2 (1 + 2f_{\text{eq}}) \right] \quad (9)$$

where the first term in square brackets describes the bulk jet kinetic

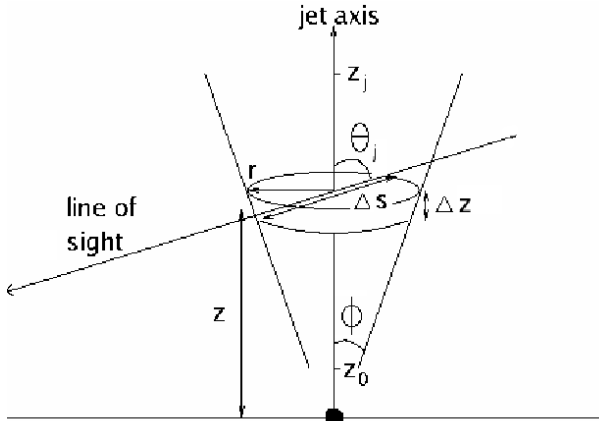


**Figure 1.** Schematic diagram of the jet geometry (not to scale). The jet radio synchrotron emission begins at a height  $z_0$  above the midplane and extends to  $z_j$ , with half opening angle  $\phi$ . It is divided into cylindrical sections of thickness  $\Delta z$  and radius  $r \approx z\phi$ . The angle between the jet axis and the line of sight is  $\theta_j$  and the path length through each cylinder is  $\Delta s$ .

energy and the second term describes the electron kinetic energy and the magnetic energy. Once the parameter  $\epsilon_j/\epsilon_a$  has been set, we use the above equation to normalize the electron number density  $N_{e,0}$  at the base of the jet. Further details of the model are described in Jolley & Kuncic (2008a).

### 3 THE BORDERLINE BLAZAR 3C 273

The well known radio-loud quasar 3C 273 ( $z = 0.158$ ) is sometimes classified as a blazar due to its strong radio jet with superluminal motion and strong flux variability. The dynamical mass of the black hole in 3C 273 has been determined from  $C_{IV}$  and  $Ly\alpha$  line widths to be  $M \approx 6.59 \times 10^9 M_\odot$  (Paltani & Türler 2005). The SED of 3C 273 exhibits a big blue bump which does not vary significantly in flux on long time scales (Paltani, Courvoisier, & Walter 1998). Any thermal disc component should be unpolarized because it is optically thick blackbody emission. However, the observed optical flux is polarized up to 2.5% (De Diego et al. 1992), providing strong evidence that jet synchrotron emission contributes to the optical emission. Jorstad et al. (2005) determined the kinematics of jets in several AGN from a three year study using the Very Long Baseline Array (VLBA). They found that the jet in 3C 273 has a Lorentz factor of  $\Gamma \approx 10$ , Doppler factor  $\delta \approx 9.5$  and an inclination angle  $\approx 6^\circ$ . We set the optically thin synchrotron spectral index  $\alpha \approx 1$ , and the equipartition factor  $f_{eq} = 1$ . The SED also has a NIR bump at  $\approx 10^{14}$  Hz. This feature is due to thermal emission from heated dust rather than synchrotron emission (e.g. Robson et al. 1986; Türler et al. 2006) and we do not model this component here.

Figure 2 shows our spectral modelling fits to the radio-UV SED of 3C 273 (data points are from Soldi et al. 2008). The dashed line is the jet-modified disc contribution only, and the solid line is the combined disc and synchrotron jet spectrum predicted by our model taking into consideration the global disc+jet energy budget. The dotted line is the best-fit standard relativistic disc spectrum predicted by Novikov & Thorne (1973). Fig. 2(a) is for the case of a non-spinning black hole ( $a = 0$ ), and Fig. 2(b) is the case for a near maximally spinning black hole ( $a = 0.97$ ). The physical parameters for the best-fit spectral models shown in Fig. 2 are presented

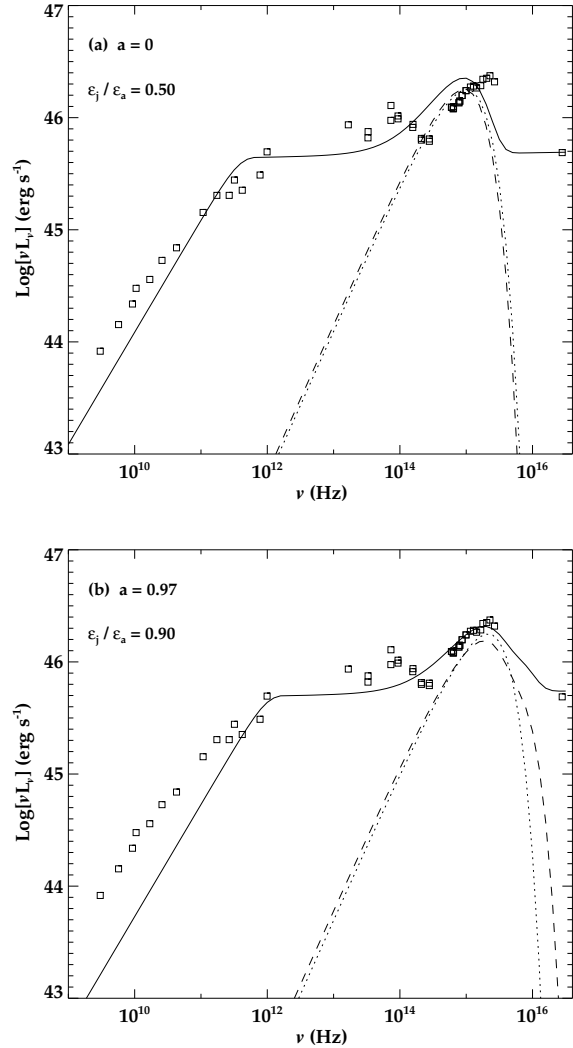


**Figure 2.** Spectral modelling fits for 3C 273, in the blazar rest frame. The dashed line is the contribution from the jet-modified accretion disc only, and the solid line is the total contribution from the synchrotron jet and the disc. The dotted line is the best-fit standard relativistic disc emission.  $a$  is the dimensionless black hole spin,  $\epsilon_j/\epsilon_a$  is the fraction of the accretion power channelled to a jet. The squares are observational data points listed in Soldi et al. (2008).

in Table 1. We model the radio synchrotron jet emission from a minimum height  $z_0 = 100r_g$  above the midplane. The jet radius at this height is  $r_{j,0} = 60r_g$  for the  $a = 0$  case and  $r_{j,0} = 17r_g$  for  $a = 0.97$ . The electron number density and magnetic field strength at the base of the jet are  $N_{e,0} \approx 7 \times 10^3 \text{ cm}^{-3}$ ,  $B_0 \approx 1 \text{ G}$  for  $a = 0$ , and  $N_{e,0} \approx 8 \times 10^5 \text{ cm}^{-3}$ ,  $B_0 \approx 5 \text{ G}$  for  $a = 0.97$ , respectively. Our predictions of the magnetic field strength at the base of the jet match those derived independently from multifrequency VLBA observations of the core (Savolainen et al. 2008).

In order to fit the observational data around  $\approx 10^{15}$  Hz, where the BBB peaks, our model predicts that the black hole must be rapidly spinning (Fig. 2 (b)). For  $a = 0$ , both the standard relativistic disc model and our jet-modified disc model are too red to adequately fit the observational data points for the tightly constrained black hole mass. The disc spectrum for a spinning black hole (Fig.

2 (b) is bluer because the last marginally stable orbit is smaller. Our results agree with Türler et al. (2006), who find evidence of a very broad  $K\alpha$  line in 3C 273, suggesting that the black hole may be rapidly spinning. We note that the predicted synchrotron jet radio emission underpredicts the observed radio emission. This is because we have not modelled radio-lobe synchrotron emission which dominates in radio-loud sources.

Table 2 compares the mass accretion rates predicted by our jet-modified disc model with that predicted by the standard disc model. Our model (Fig. 2, dashed lines) predicts a higher  $\dot{M}_a$  for 3C 273 than the standard model predicts (Fig. 2, dotted lines) for the same disc luminosity. This is because our model self-consistently takes into account the additional accretion power used to power the jet. As a result, the disc efficiencies predicted by our model are lower and  $\dot{m}$  is higher.

#### 4 HIGH REDSHIFT BLAZARS

The UV/Optical Telescope (UVOT) (Roming et al. 2005) aboard the SWIFT satellite was used to observe several high redshift blazars, including PKS 0836+710 ( $z = 2.172$ ), 2149-307 ( $z = 2.345$ ), 0537-286 ( $z = 3.104$ ), and B2 0743+25 ( $z = 2.979$ ) (also known as SWIFT J0746.3+2548) (Sambruna et al. 2006, 2007). These sources exhibit strong emission lines in their optical spectra and thus, are classified as FSRQs. Strong X-ray emission and rapid variability indicate that the radiation is relativistically beamed. In the optical-UV, the lack of variability is consistent with radiation from a different component such as thermal emission from an accretion disc. Indeed, the optical-UV emission in PKS 0836+710 was found to have a polarization of  $1.1 \pm 0.5\%$  (Impey & Tapia 1990). This is lower than that usually observed in other jet-dominated blazars, suggesting that the BBB is predominantly thermal in origin, with a small synchrotron jet contribution.

Our spectral modelling results for these four blazars are shown in Figure 3. The total jet+disc spectrum is shown for a mass of  $M = 5 \times 10^9 M_\odot$  (solid line) and for  $M = 10^{10} M_\odot$  (dashed line) (e.g. see Yu-ying et al. 2008; Vestergaard et al. 2008; Netzer et al. 2007). The inclination of the jet to our line of sight is  $\theta = 3^\circ$  (Sambruna et al. 2007). The jet Lorentz factor is  $\Gamma_j = 5$ , corresponding to a Doppler factor of  $\delta \approx 9$ . We find that the  $M = 5 \times 10^9 M_\odot$  case requires  $a = 0$  because a high-spin disc produces a bluer spectrum that peaks past the UVOT data points. Similarly, the maximum possible spin for the  $M = 10^{10} M_\odot$  case is  $a = 0.6$ . Our jet-modified accretion disc model predicts a maximum  $\epsilon_j/\epsilon_a \approx 0.50$  for  $a = 0$  and  $\epsilon_j/\epsilon_a \approx 0.70$  for  $a = 0.6$ . The optically thin synchrotron spectral index is set to  $\alpha = 1.50$  to be consistent with the UV fall-off, and the equipartition factor  $f_{\text{eq}} = 1$ . Other parameters are listed in Table 1. We deduce the initial height of the radio synchrotron jet emission to be  $z_0 = 500r_g$  with radius  $r_{j,0} = 300r_g$ , and the electron number density and magnetic field strength at the base of the jet are  $N_{e,0} \approx 1-9 \times 10^2 \text{ cm}^{-3}$  and  $B_0 \approx 0.5-1\text{G}$ , respectively.

As in the previous case for 3C 273, Table 2 shows that the mass accretion rates  $\dot{M}_a$  inferred for these high-redshift blazars are all consistently higher than those predicted by the standard relativistic disc model. This is because, for a given luminosity, additional accretion power is needed to self-consistently account for the jet.

#### 5 DISCUSSION AND CONCLUSIONS

The strongly beamed jet emission of blazars and limited optical monitoring data make fitting a thermal disc spectral component difficult. Nevertheless, the presence of a strong jet in blazars suggests that thermal disc emission in these sources should be strongly jet-modified, and that the mass accretion rates can be substantially higher (by at least a factor of  $\approx 2$ ) than those inferred from standard accretion disc models (which assume all the accretion power is locally dissipated in the disc). In the case of 3C 273,  $\dot{M}_a$  may be more than a factor of 7 higher than would be inferred from the standard model. Previous attempts to model the optical emission from 3C 273 using various accretion models have met with limited success (see e.g. Blaes et al. 2001 and references therein). Magnetic torques and the effects of the jet are neglected, resulting in high radiative efficiencies, low mass accretion rates and poor fits to the observed spectra. In order to successfully reproduce the BBB in 3C 273, it is necessary to self-consistently include the presence of the jet and the magnetic torques responsible for coupling the jet to the disc.

We have considered a new accretion model which incorporates magnetic disc-jet coupling and which takes into consideration energy partitioning between thermal (disc) emission and bulk kinetic (jet) energy. Our model predicts that the nearby borderline blazar 3C 273 is powered by a rapidly spinning ( $a = 0.97$ ) black hole accreting at a rate  $\dot{M} \approx 20 M_\odot \text{ yr}^{-1}$ . Conversely, we also find that the high redshift blazars PKS 0836+710, PKS 2149-307, B2 0743+25 and PKS 0537-286, are likely to harbour a low-spin ( $a < 0.6$ ) black hole. Our model predicts that these high redshift sources are accreting at much higher rates of approximately  $50 - 200 M_\odot \text{ yr}^{-1}$ . These results are consistent with cosmological spin evolution scenarios (see e.g. Jolley & Kuncic 2008c and references therein). The black hole in 3C 273 ( $z = 0.158$ ) may have been spun up as a result of sustained, systematic accretion. At high redshift, mergers and/or episodic accretion of randomly oriented material mitigates spin evolution (see e.g. Berti & Volonteri 2008 and references therein).

Unlike 3C 273, the masses of the black holes powering the high redshift blazars are poorly constrained. Our spectral modelling results suggest that  $M \approx 5 \times 10^9 M_\odot$  is the minimum black hole mass in these blazars. Lower values of  $M$  would result in accretion disc spectra that are too blue with respect to the observational data, even when  $a = 0$ . For  $M = 10^{10} M_\odot$ , we find  $a \approx 0.6$ . As values of  $M \gtrsim 10^{10} M_\odot$  are ruled out by observations (for example, see Yu-ying et al. 2008; Vestergaard et al. 2008; Netzer et al. 2007 and references therein), the black hole spin must be  $a \leq 0.6$  for these sources.

The presence of strong jets enhances the accretion growth of black hole mass. This is because jets enhance the rate of angular momentum transport and hence, the mass accretion rate (Jolley & Kuncic 2008a). Thus, the observed correlation between radio loudness and black hole mass (see e.g. Metcalf & Magliocchetti 2006 and references therein) can be explained by jet-enhanced accretion growth (Jolley & Kuncic 2008c). For the zero spin case, the mass accretion rates found using our jet-modified accretion disc model are approximately twice that predicted by a standard accretion disc for the same disc luminosity (see Table 2). This is because half the accretion power is channelled to the jet. As a result, the disc radiative efficiency is half that predicted by the standard model.

More generally, our results indicate that jet activity is responsible for the changes in radiative efficiency that result in different spectral modes and accretion states in AGN and galactic x-ray bina-

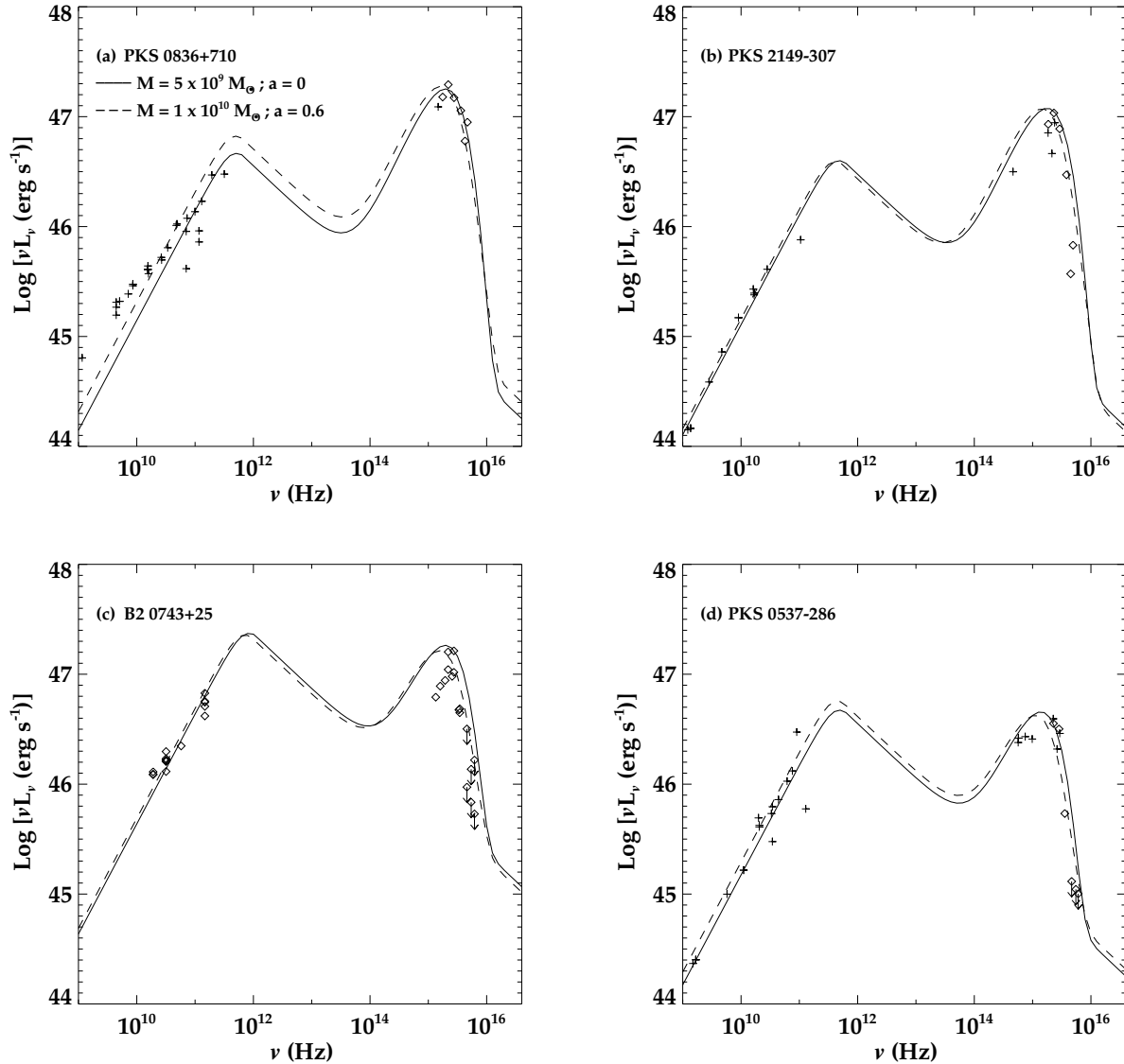


**Figure 3.** Spectral fits for the UVOT/SWIFT blazars in the blazar rest frame. The solid line is the total jet+disc spectrum for a black hole of mass  $M = 5 \times 10^9 M_\odot$  and spin  $a = 0$ , and the dashed line is for  $M = 10^{10} M_\odot$  and spin  $a = 0.6$ . The observational data points are from Sambruna et al. (2006, 2007) (diamonds) and from NED (plus signs).

ries (Jester 2005). Indeed, we have demonstrated in previous work (Jolley & Kuncic 2008a,b) that jet-modified disc accretion can successfully explain low luminosity AGN. Furthermore, consideration of energy partitioning between the jet and disc requires the disc radiative efficiency to be less than that predicted by accretion models that neglect this partitioning. Hence, our values of the dimensionless mass accretion rate  $\dot{m}$  are higher than those predicted by standard accretion models.

In future work, the accretion parameters predicted by our model can be used to derive further information about the disc-jet coupling, such as the magnetic field strength required to launch jets (Bicknell & Li 2007), or the black hole mass-growth history and spin evolution. Our spectral model could also be extended to predict the x-ray emission resulting from Comptonisation of disc photons in the jet. This may explain why the observed jet x-rays in

3C 273 are not correlated with the jet radio synchrotron emission (Courvoisier et al. 1987; Soldi et al. 2008). Tighter observational constraints on black hole masses and more optical monitoring of blazars to obtain more data in their low state, would allow us to better constrain their accretion and black hole properties.

#### ACKNOWLEDGMENTS

E.J.D.J acknowledges support from a University of Sydney Post-graduate Award. The authors would like to thank an anonymous referee for useful comments that greatly improved the paper. This research has made use of the NASA/IPAC Extragalactic Database (NED) which is operated by the Jet Propulsion Laboratory, California Institute of Technology, under contract with the National Aeronautics and Space Administration.

**Table 1.** Parameters used in the spectral fits shown in Figs. 2 and 3 for our disc+jet model. For comparison, the radiative efficiency for the standard relativistic disc model is  $\epsilon_d = 0.06$  for  $a = 0$ ,  $\epsilon_d = 0.10$  for  $a = 0.60$ , and  $\epsilon_d = 0.25$  for  $a = 0.97$ . See text for a description of other parameters.

Fig.	$z$	$M$ ( $\times 10^9 M_\odot$ )	$a$	$L_d/L_{\text{Edd}}$	$\epsilon_d$	$\epsilon_j/\epsilon_a$	$\dot{M}_a$ ( $M_\odot \text{ yr}^{-1}$ )	$\Gamma_j$	$\langle \gamma \rangle$	$P_j^{\text{obs}}$ ( $\times 10^{47} \text{ erg s}^{-1}$ )	
3C273	1(a)	0.158	6.59	0	0.05	0.03	0.50	22	10	60	0.6
	1(b)		6.59	0.97	0.05	0.03	0.90	23	10	9	0.7
PKS 0836+710	2(b)	2.172	5	0	0.60	0.03	0.50	222	5	38	1.8
			10	0.6	0.32	0.03	0.7	228	5	27	2.6
PKS 2149-307	2(c)	2.345	5	0	0.40	0.03	0.50	148	5	45	1.6
			10	0.6	0.020	0.03	0.7	143	5	30	2.5
B2 0743+25	2(d)	2.979	5	0	0.60	0.03	0.50	222	5	60	9.3
			10	0.6	0.27	0.03	0.7	192	5	42	9.0
PKS 0537-286	2(a)	3.104	5	0	0.15	0.03	0.50	56	5	83	1.9
			10	0.6	0.07	0.03	0.7	50	5	60	2.3

**Table 2.** Mass accretion rates predicted by our jet-modified disc and by the standard relativistic accretion disc model. The dimensionless black hole spin is  $a$ , the mass accretion rate  $\dot{M}_a$  is defined in Eq. (6), and the dimensionless mass accretion rate  $\dot{m}$  is defined in Eq. (7).

$z$	$M$ ( $\times 10^9 M_\odot$ )	$a$	jet-modified disc		standard disc		
			$\dot{M}_a$ ( $M_\odot \text{ yr}^{-1}$ )	$\dot{m}$	$\dot{M}_a$ ( $M_\odot \text{ yr}^{-1}$ )	$\dot{m}$	
3C273	0.158	6.59	0	22	1.5	12	0.8
		6.59	0.97	23	1.6	3	0.2
PKS 0836+710	2.172	5	0	222	20.1	117	10.5
		10	0.6	228	10.3	75	3.4
PKS 2149-307	2.345	5	0	148	13.4	78	7.0
		10	0.6	143	6.4	47	2.1
B2 0743+25	2.979	5	0	222	20.1	117	10.5
		10	0.6	192	8.7	64	2.9
PKS 0537-286	3.104	5	0	56	5.0	29	2.6
		10	0.6	50	2.3	17	0.7

**REFERENCES**

- Agol E., Krolik J., 2000, *ApJ*, 528, 161  
Berti E., Volonteri M., 2008, *ApJ*, 684, 822  
Bicknell G.V., Li J., 2007, *ApSS*, 311, 275  
Blaes O., Hubeny I., Agol E., Krolik J., 2001, *ApJ*, 563, 560  
Blandford R.D., Königl A., 1979, *ApJ*, 232, 34  
Blandford R.D., Payne D.G., 1982, *MNRAS*, 199, 883  
Courvoisier T.J.-L., Turner M.J.L., Robson E.I. et al., 1987, *A&A*, 176, 197  
De Diego J.A., Perez E., Kidger M.R., Takalo L.O., 1992, *ApJ*, 396, L19  
Fossati G., Maraschi L., Celotti A., Comastri A., Ghisellini G., 1998, *MNRAS*, 299, 433  
Freeland M., Kuncic Z., Soria R., Bicknell G.V., 2006, *MNRAS*, 372, 630  
Ghisellini G., Celotti A., Fossati G., Maraschi L., Comastri A., 1998, *MNRAS*, 301, 451  
Impey C.D., Tapia S., 1990, *ApJ*, 354, 124  
Jester S., 2005, *ApJ*, 625, 667  
Jolley E.J.D., Kuncic Z., 2008a, *ApJ*, 676, 351  
Jolley E.J.D., Kuncic Z., 2008b, *ApSS*, 310, 327  
Jolley E.J.D., Kuncic Z., 2008c, *MNRAS*, 386, 989  
Jorstad S.G., Marscher A.P., Lister M.L. et al., 2005, *AJ*, 130, 1418  
Kuncic Z., 1999, *PASP*, 111, 954  
Kuncic Z., Bicknell G.V., 2004, *ApJ*, 616, 669  
Kuncic Z., Bicknell G.V., 2007a, *ApSS*, 311, 127  
Kuncic Z., Bicknell G.V., 2007b, *MPLA*, 22, 1685  
Maraschi L., Tavecchio F., 2003, *ApJ*, 593, 667  
Metcalf R.B., Magliocchetti M., 2006, *MNRAS*, 365, 101  
Netzer H., Lira P., Trakhtenbrot B., Shemmer O., Cury L., 2007, *ApJ*, 671, 1256  
Novikov I.D., Thorne K.S., 1973, *Black Holes*, New York Gordon & Breach  
Page D.N., Thorne K.S., 1974, *ApJ*, 191, 499  
Paltani S., Courvoisier T.J.-L., Walter R., 1998, *A&A*, 340, 47  
Paltani S., Türler M., 2005, *A&A*, 435, 811  
Perlman E.S., Addison B., Georganopoulos M., Wingert B., Graff P., 2008, *PoS*, in press  
Pringle J.E., Rees M.J., 1972, *A&A*, 21, 1  
Raiteri C.M., Villata M., Larionov V.M. et al., 2007, *A&A*, 473, 819  
Robson E.I., Gear W.K., Brown L.J.M., Courvoisier T.J.-L., Smith M.G., 1986, *Nature*, 323, 134  
Romig P.W.A., Kennedy T.E., Mason K.O. et al., 2005, *SSR*, 120, 95  
Samburina R.M., Markwardt C.B., Mushotzky R.F. et al., 2006,

- ApJ, 646, 23
- Sambruna R.M., Tavecchio F., Ghisellini G. et al., 2007, ApJ, 669, 884
- Savolainen T., Wiik K., Valtaoja E., Tornikoski M., 2008, ASP, 386, 451
- Shakura N.I., Sunyaev R.A., 1973, A&A, 24, 337
- Shang Z., Brotherton M.S., Green R.F. et al., 2005, ApJ, 619, 41
- Soldi S., Türler M., Paltani S. et al., 2008, A&A, 486, 411
- Tavecchio F., Maraschi L., Ghisellini G. et al., 2000, ApJ, 543, 535
- Türler M., Chernyakova M., Courvoisier T.J.-L. et al., 2006, A&A, 451, L1
- Urry C.M., Padovani P., 1995, PASP, 107, 803
- Vestergaard M., Fan X., Tremonti C.A., Osmer P.S., Richards G.T., 2008, ApJ, 674, L1
- Willott C.J., Rawlings S., Blundell K.M., Lacy M., 1999, MNRAS, 309, 1017
- Yu-ying B., Xiong Z., Luo-en C., Hao-jing Z., Zhao-yang P., Yong-gang Z., 2008, Ch. A&A, 32, 351